ELSEVIER

Catalysis Today 66 (2001) 467–474

CATALYSIS TODAY

www.elsevier.com/locate/cattod

Modelling of a photocatalytic reactor with a fixed bed of supported catalyst

A. Alexiadis*, G. Baldi, I. Mazzarino

Dipartimento di Scienza dei Materiali e Ing. Chimica, Politecnico di Torino, c. Duca degli Abruzzi, 24, 10129 Turin, Italy

Abstract

This work intends to develop a mathematical model of a fixed bed reactor and tests this model with experimental data. For this reason, we introduce some specific knowledge about light absorption from the catalyst, about the hydrodynamic interpretation of the reactor and the kinetic behaviour of photocatalytic reactions. Afterwards, we summarise this information and set up a complex mathematical model. We use this model in order to identify the kinetic constants of some reactions. We also formulate some simplified models to be used in particular circumstances and we compare the results of the complex model and the simplified models. Moreover, we compare experimental data of conversion and the results estimated with our model. © 2001 Elsevier Science B.V. All rights reserved.

Keywords: Water pollution; Photocatalytic oxidation; Supported photocatalyst

1. Introduction

In the last years, the problems related to the environmental protection became one of the main challenges for the reaction engineering research. In this field, the innovative water treatments are one of the main fields of work. The photocatalytic and photochemical processes show interesting features. The operating conditions are not severe and usually there is no need to add chemical reactants which could generate secondary pollution phenomena. In the last years, many studies proved that a large number of pollutants can be oxidised in this way. These studies, however, were done in slurry reactors where small size catalyst particles were suspended in liquid phase. This solution presents some problems: scattering and absorption on the solid particles limit the penetration of the UV light and the efficiency of the reactor. Moreover, the purified water must be filtered to remove the catalyst. To overcome these problems, photocatalytic reactors with supported catalyst have been experimentally tested [9].

In this work, a mathematical model of a fixed bed photocatalytic reactor was developed. The reactor configuration is tubular with an axial cylindrical UV lamp. The photocatalyst (TiO_2) is supported on Rashing rings of UV transparent material (quartz). Equations describing the radiant field, the reaction kinetics and the fluid dynamics are the base of the reactor model.

2. Radiant field

The kinetic constants of the photocatalytic processes depend on the absorbed light energy. The experimental tests show no conversion in the absence of the activating radiation. For this reason, we need a mathematical description of radiant field and the behaviour of light rays. The goal of any theoretical description is to evaluate the parameter e^a, i.e. the local volumetric rate of energy absorption (LVREA).

---

* Corresponding author.

E-mail address: alexiadi@athena.polito.it (A. Alexiadis).

0920-5861/01/$ – see front matter © 2001 Elsevier Science B.V. All rights reserved.
PII: S0920-5861(01)00255-3

Nomenclature

a_{cat}	specific area of catalyst
a_{GAS}	specific area of bubble
c_{dark}	concentration of the pollutant in the dark zone
c_{light}	concentration of the pollutant in the light zone
c_{L}	concentration of the pollutant in the bulk of liquid phase
c_{S}	concentration of the pollutant on the catalyst surface
c_0	concentration of the pollutant at the inlet of the reactor
d_{p}	catalyst particle diameter
d_{r}	bubble diameter
D_{L}	gas liquid diffusivity
D_{r}	radial dispersion
e^{a}	local volumetric rate of energy absorption (LVREA)
E_{L}	lamp energy (we considered only a specific λ)
h_{up}	liquid hold-up
k_{L}	mass transfer coefficient (liquid–gas)
k_{s}	mass transfer coefficient (liquid–catalyst surface)
$K_{\text{L–D}}$	mass transfer coefficient between light and dark zone
L_{L}	lamp length
O_2^{cat}	concentration of the oxygen on the catalyst surface
O_2^{gas}	concentration of the oxygen in the gas phase
$\text{O}_2^{\text{light}}$	concentration of the oxygen in the light zone
O_2^{liq}	concentration of the oxygen in the bulk of liquid phase
R_{A}	rate of reaction
$\bar{R}_{\text{A}}$	average rate of reaction in the light zone
R_{R}	reactor radius
R_0	lamp radius
s	linear coordinate along ω
v_{g}	interstitial velocity of gas phase
v_{L}	interstitial velocity of liquid phase
v_0	stoichiometric coefficient of reaction
W_{LAMP}	power of the lamp

Greek letters

ε	bed porosity
μ_{g}	gas viscosity
μ_{L}	liquid viscosity
μ_v	Lambert–Beer coefficient
ρ	distance from the considered point to the lightening element
ρ_{g}	gas density
ρ_{L}	liquid density
σ_v	scattering coefficient
Φ_{gas}	gas flow
Φ_{liq}	liquid flow
ω	direction of the incident ray
ω'	the direction of the scattered ray

In the last 30 years, many authors studied the propagation of light in an absorbent medium and there are several models of the radiant field available in the literature. We have tested three of these models.

As a first approach, the simplest model, the LSPP (line source model with emission in parallel planes) was used. The model considers a thread-like lamp; the emission is isotropic and orthogonal to the lamp axe. So the balance of light energy leads to the following result [2]:

$$e^{\text{a}} = \int_{v=0}^{v=\infty} \mu_v \frac{\mathrm{d}E_v}{2\pi L_{\text{L}}} \frac{1}{r} \exp\left(-\int_{R_0}^{r} \mu_v \,\mathrm{d}r\right) \tag{1}$$

For a monochromatic emission and a simple geometry like in our case:

$$e^{\text{a}} = \mu_v \frac{E_{\text{L}}}{2\pi L_{\text{L}}} \frac{1}{r} \exp\left(-\int_{R_{\text{L}}}^{R_{\text{R}}} \mu_v \,\mathrm{d}r\right) \tag{2}$$

If, nevertheless, the geometry is still cylindrical but the emission zone is shorter than the reactor length, it is not correct use of the LSPP model. In fact, the LSPP model sees the light propagation as many coaxial cylinders and does not include propagation of energy in the zone above and under the lamp. This is not satisfactory if the reaction zone is longer than the lamp. One need in this case is a more realistic model for modelling the radiant field. A more complex model is the so-called LSSE (line source model with spherical emission). In this case, the lamp is still considered thread-like but the emission is spherical. The energy

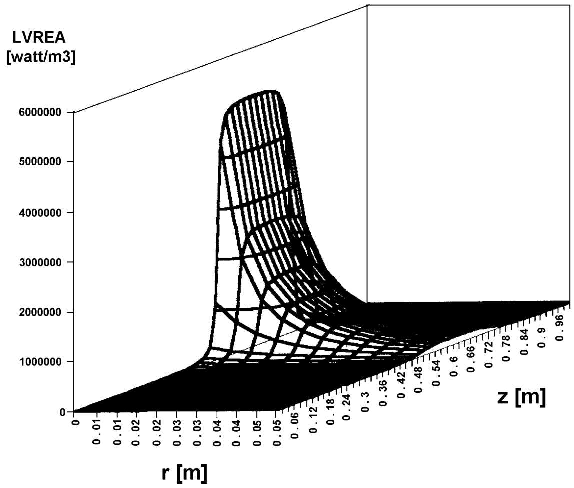

Fig. 1. Radiant field with LSSE model.

balance gives

$$e^{\mathrm{a}} = \int_{v=0}^{v=\infty} \mu_v \frac{\mathrm{d}E_v}{4\pi L_{\mathrm{L}}} \int_0^{L_{\mathrm{L}}} \frac{1}{r^2} \exp\left(-\int_{R_0}^{r} \mu_v \,\mathrm{d}r\right) \mathrm{d}z \tag{3}$$

Practically, the LVREA consists in the integral energy contribute, with spherical emission, of every point of the lamp. Fig. 1 shows the result of the integration.

Both LSPP and LSSE models are well known and reported in the literature [2,3]. In the case of a tubular configuration like that investigated in this work, these models are substantially equivalent.

The third tested case takes into consideration directly the balance of energy of light [13]. The behaviour of the photons generated from the lamp, in fact, is more complex than what we until now have considered. The energy of the lamp can be both absorbed and reflected by the catalyst surface and this originates the phenomena of *scattering*. The scattering could be both elastic (when λ changes) and inelastic (when λ does not change). The balance of energy, considering only the case of inelastic scattering, is [13]

$$\frac{\mathrm{d}I_{v\omega}}{\mathrm{d}s} = -(\mu_\lambda + \sigma_\lambda) I_{v\omega} + \frac{\sigma_\lambda}{4\pi} \int_{4\pi} I_{v\omega} p_\lambda(\omega', \omega) \,\mathrm{d}\Omega \tag{4}$$

where s is the linear coordinate along ω (direction of the incident ray), ω' the direction of the scattered ray, σ_v the scattering coefficient, $p_\lambda(\omega', \omega)$ the function of phase, and represents the probability that a ray with direction ω' is scattered on an ω direction. The first term of the aforementioned equation is the Lambert–Beer relation, the second, however, represents the scattered energy from every direction ω' to ω. We used *Monte Carlo* approaches for solving Eq. (4) [14].

3. Reactor model

The examined system was considered pseudo-homogeneous assuming that the reaction takes place only on the catalyst's external surface.

Thus, the equations of mass balance for the pollutant are

$$\begin{aligned} &-v_{\mathrm{L}} \frac{\partial c_{\mathrm{L}}}{\partial z} + \frac{D_{\mathrm{r}}}{r} \frac{\partial c_{\mathrm{L}}}{\partial r} + D_{\mathrm{r}} \frac{\partial^2 c_{\mathrm{L}}}{\partial r^2} + R_{\mathrm{A}} \frac{a_{\mathrm{cat}}}{h_{\mathrm{up}}} = 0, \\ &k_{\mathrm{s}}(c_{\mathrm{L}} - c_{\mathrm{S}}) a_{\mathrm{cat}} \,\mathrm{d}V = R_{\mathrm{A}} a_{\mathrm{cat}} \,\mathrm{d}V, \\ &R_{\mathrm{A}} = f(c_{\mathrm{S}}, \mathrm{O}_2^{\mathrm{cat}}, e^{\mathrm{a}}) \end{aligned} \tag{5}$$

and for the oxygen:

$$\begin{aligned} &-v_{\mathrm{L}} \frac{\partial \mathrm{O}_2^{\mathrm{liq}}}{\partial z} + \frac{D_{\mathrm{r}}}{r} \frac{\partial \mathrm{O}_2^{\mathrm{liq}}}{\partial r} + D_{\mathrm{r}} \frac{\partial^2 \mathrm{O}_2^{\mathrm{liq}}}{\partial r^2} + \cdots \\ &\quad + R_{\mathrm{O}_2} \frac{a_{\mathrm{cat}}}{h_{\mathrm{up}}(1-\varepsilon)} - k_{\mathrm{L}}(\mathrm{O}_2^{\mathrm{gas}} - \mathrm{O}_2^{\mathrm{liq}}) \frac{a_{\mathrm{GAS}}}{h_{\mathrm{up}}} = 0, \\ &k_{\mathrm{s}}(\mathrm{O}_2^{\mathrm{liq}} - \mathrm{O}_2^{\mathrm{cat}}) a_{\mathrm{cat}} \,\mathrm{d}V = R_{\mathrm{O}_2} a_{\mathrm{cat}} \,\mathrm{d}V, \\ &R_{\mathrm{O}_2} = v_0 R_{\mathrm{A}}, \quad A + v_0 \mathrm{O}_2 \rightarrow P \end{aligned} \tag{6}$$

The boundary conditions are

$$\begin{aligned} &z = 0, \quad R_0 \le r \le R, \quad c_{\mathrm{L}} = c_0, \quad z > 0, \\ &r = R_0, \quad \frac{\partial c_{\mathrm{L}}}{\partial r} = 0, \qquad z > 0, \quad r = R, \quad \frac{\partial c_{\mathrm{L}}}{\partial r} = 0 \end{aligned} \tag{7}$$

$$\begin{aligned} &z = 0, \quad R_0 \le r \le R, \quad \mathrm{O}_2^{\mathrm{liq}} = \mathrm{O}_{2,0}^{\mathrm{liq}}, \qquad z > 0, \\ &r = R_0, \quad \frac{\partial \mathrm{O}_2^{\mathrm{liq}}}{\partial r} = 0, \qquad z > 0, \\ &r = R, \quad \frac{\partial \mathrm{O}_2^{\mathrm{liq}}}{\partial r} = 0 \end{aligned} \tag{8}$$

k_{s} and k_{L} values were calculated by literature correlation (see [5,6] for k_{s} and [10,11,15] for k_{L}).

The aforementioned correlations of k_L yield very different values: Saada gives the lowest, the values obtained by Reiss are about one order in magnitude bigger than Saada's and finally those obtained by Specchia are one order in magnitude bigger than those by Reiss. The one of Specchia et al. [15] was chosen for k_L, because closer to the conditions adopted in this work. For the same reason, the correlation by Mochizuki was adopted for k_s.

Hydrodynamics and reaction kinetics must be combined with the balance of radiant energy. This is the reason why our system has particular characteristics; in fact, radial gradients can play an important role. Kinetic constants, and the rate of reaction, depend on the absorbed light and, consequently, they changes with the position. So, radial gradients of concentration may play a significant role, due to large radial decrease of the intensity of light field. For this reason, we introduce the radial dispersion term D_r in the model.

4. Chemical reaction

A complex rate equation developed by Minero [4] assuming a detailed reaction mechanism model was used:

$$R_A = \left(\frac{X}{Z}e^a\right)\left((-4Y-\beta)\left(\left(\frac{4}{\beta}\right)(Z(X+8Y-\beta) - X^2(X+4Y-\beta)+8Y^2(\beta+4X))^{1/2}\right)\right) \quad (9)$$

where $\beta = (X(X+4Y))^{1/2}$, $X = K_1 O_2^{cat}$, $Y = K_2 C_{cat}$, $Z = K_3 e^a$, and K_1, K_2, K_3 are the kinetic constants.

This kinetic rate equation approximates, better than a simpler Langmuir, the photochemical reaction in liquid phase. In fact, the reaction rate may present maximum, as a function of concentration of the organic pollutant, that a Langmuir type approach cannot provide.

5. Radial dispersion

As said before, the radial dispersion term D_r is present in Eqs. (5) and (6). This value is very important because considerations about radial profile and optimal radial thickness of the reactor are based on D_r. We estimate the value of $D_r = 10^{-6}\,m^2/s$ [1] but is useful to note the dependence of the conversion from this parameter (see Fig. 2).

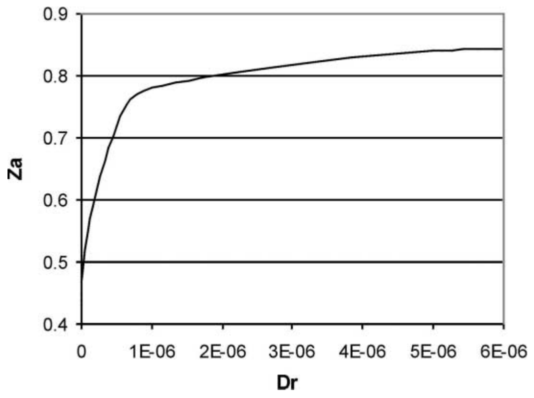

Fig. 2. Conversion in the reactor varying D_r (m^2/s) with a thickness of the fixed bed of 5 cm.

We can see how, increasing the radial dispersion, the profile of the curve in Fig. 2 becomes flat. When D_r is low, there is a bad mass transfer between the zone close to the lamp, where the kinetics rate is high, and the bulk, where the kinetics rate is low. So, near the lamp, the organic pollutant concentration falls quickly to low values and to achieve further conversion is difficult. When radial dispersion is high, on the other hand, a good mass transfer between the two zones permits higher values of the conversion. However, increasing D_r over a certain value, the radial mass transfer becomes uncontrollable with respect to other parameters and the conversion cannot increase further. Of course, we obtain Fig. 2 numerically, varying D_r but fixing all other parameters. If we increase the thickness of the catalytic bed, for instance, we need a higher radial dispersion to get again a flat radial profile of concentration. Also, the relation between D_r and the chemical rate of reaction are important. A high rate of reaction means a more important influence of the radial mass transfer and, on the other hand, if the reaction rate is slow, the opposite happens. So it is impossible to make generic consideration about the radial behaviour of the reactor, without considering directly the radial dispersion.

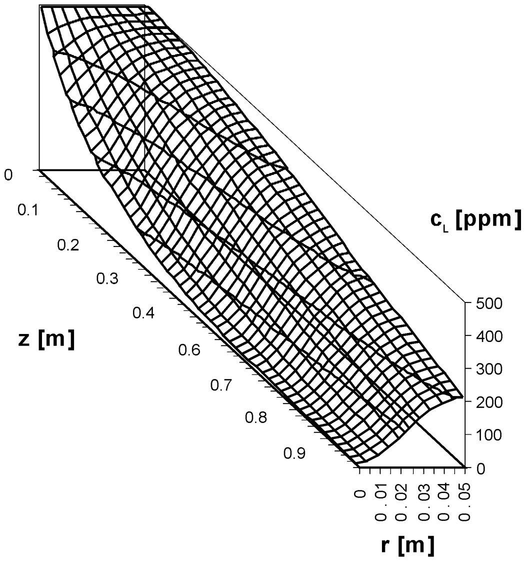

Fig. 3. Outline of pollutant concentration along the reactor (we used $D_r = 10^{-7}\,m^2/s$ in order to accentuate the radial profile).

6. Numerical computation

The rate equation of Eq. (9) was used as the generation term in the differential equation of local mass balance, which was solved by a finite difference method. In this way, one obtains a qualitative outline of c_L.

The results of the mathematical simulation suggest the existence of two different zones in the reactor: the light and the dark zone (Figs. 3 and 4). The first is the zone near the lamp, where most of the light is absorbed and the conversion is high. The thickness of this zone is called *optical thickness* and it is inversely proportional to the Lambert–Beer coefficient.

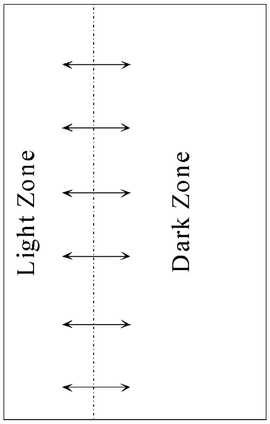

Fig. 4. The two zones in the reactor.

The second zone is the remaining part of the reactor. A very small fraction of the light energy arrives here, because most of the photons are absorbed in the previous one. When the Lambert–Beer coefficient is high, an increase of the lamp power gives rise to a higher reactivity in the light zone. However, the thickness of this zone remains practically the same, according to the calculations. One can see that the thickness of the light zone depends on the Lambert–Beer coefficient, but the reactivity in this zone is affected by the power of the lamp. If the reactor radius is smaller than the optical thickness, it is useless to increase the power of the lamp above a certain value because when in the light zone the conversion is nearly total, no further increase can occur. In the dark zone, the reactivity is very low, but there is mass transfer between the two zones so that reactants are fed to the reactive part of the catalytic bed from the dark zone. The mechanism of this transport can be either diffusive or turbulent. A radial mass dispersion parameter D_r is, as said before, used to summarise all these phenomena.

7. Simplified models

One of the main goals of the reactor simulation by mathematical model is to identify the kinetic constants of the chemical process. This result can be obtained by fitting experimental data conversions. In order to save computing time and to achieve preliminary results, the reactor model can be simplified by considering special conditions. Two limit cases have been considered in this work: small and large optical thickness ($s_{opt} = \mu_v^{-1}$) values.

7.1. Small radiation penetration

In this case, the diameter of the reactor is much higher than the penetration depth of the activating radiation and most of the light is absorbed in a thin layer around the radiation source. Assuming a linear decay of the radiant field in the light zone, it is easy to calculate the average value of light energy in this

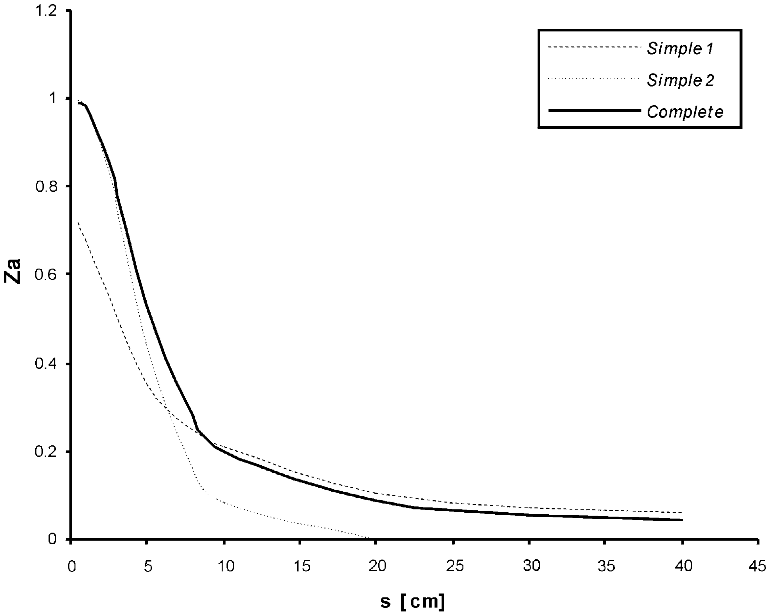

Fig. 5. Comparison between the results performed by simplified and complete reactor models. Simple 1: high radiation penetration model, simple 2: small radiation penetration model. Operative conditions: $\mu_v = 30\,\mathrm{m}^{-1}$, $\sigma_v = 120\,\mathrm{m}^{-1}$, $\Phi_{\mathrm{liq}} = 25\,\mathrm{cm}^3/\mathrm{min}$, $\Phi_{\mathrm{gas}} = 2\,\mathrm{l/min}$ and $c_0 = 500\,\mathrm{ppm}$.

volume. The only role of the dark zone is to supply the light zone with the reactants.

The mass balance for the pollutant is

$$-v_{\mathrm{L}}\frac{\partial c_{\mathrm{light}}}{\partial z} + \bar{R}_{\mathrm{A}}\frac{a_{\mathrm{cat}}}{h_{\mathrm{up}}} - K_{\mathrm{L-D}}(c_{\mathrm{light}} - c_{\mathrm{dark}}) = 0,$$
$$-v_{\mathrm{L}}\frac{\partial c_{\mathrm{dark}}}{\partial z} + K_{\mathrm{L-D}}(c_{\mathrm{light}} - c_{\mathrm{dark}}) = 0 \qquad (10)$$

The expression $K_{\mathrm{L-D}}(c_{\mathrm{light}} - c_{\mathrm{dark}})$ gives the key reactant mass transfer. Under these conditions, the general balance equation can be simplified and the radial terms disappears. However, the radial terms are not actually neglected since it is hidden in the $K_{\mathrm{L-D}}(c_{\mathrm{light}} - c_{\mathrm{dark}})$ term. It is important to identify the value of the coefficient $K_{\mathrm{L-D}}$. We assumed this parameter to be expressed by correlations like $Sh = \mathrm{constant}\,Re^a\,Sc^b$. The constants a and b are determined by imposing the condition that both the complete and the simplified model converge at the same results of conversion.

The relation $Sh = 21.5Re^{0.1}\,Sc^{1.85}(R_0/s_{\mathrm{opt}})^{1.6}$, where s_{opt} is the optical thickness (μ_v^{-1}) and R_0 the internal radius of the reactor was found to fit this condition.

7.2. High radiation penetration

In this case, the depth of penetration of the radiation is comparable with the reactor diameter. The entire reactor is a light zone and it is possible to assume an average constant value of the radiant field. The balance equation can be simplified also because radial mass transfer can be neglected.

$$-v_{\mathrm{L}}\frac{\partial c_{\mathrm{light}}}{\partial z} + \bar{R}_{\mathrm{A}}\frac{a_{\mathrm{cat}}}{h_{\mathrm{up}}(1-\varepsilon)} = 0,$$
$$-v_{\mathrm{L}}\frac{\partial \mathrm{O}_2^{\mathrm{light}}}{\partial z} + v_0\bar{R}_{\mathrm{A}}\frac{a_{\mathrm{cat}}}{h_{\mathrm{up}}(1-\varepsilon)}$$
$$+k_{\mathrm{L}}(\mathrm{O}_2^{\mathrm{gas}} - \mathrm{O}_2^{\mathrm{light}})\frac{a_{\mathrm{GAS}}}{h_{\mathrm{up}}(1-\varepsilon)} = 0 \qquad (11)$$

The light zone is considered to be perfectly mixed.

The plot of Fig. 5 clearly shows that the first simple model can be used in the case of small bed thickness and the second for the high one. Only in the case of mid-range values of the depth of penetration of the activating radiation, the complete model must be used.

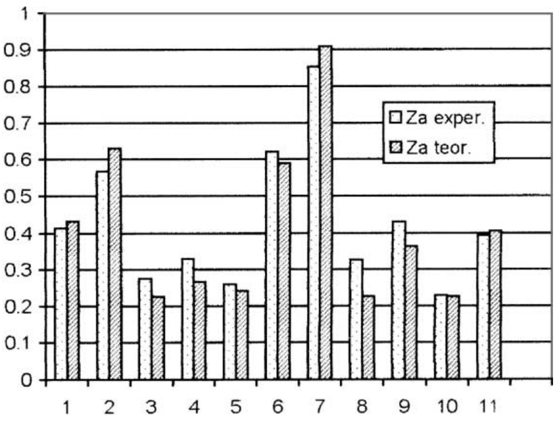

Fig. 6. Comparison between theoretical (complex model) values and experimental results.

8. Kinetic constants identification

The above described models were used to identify the kinetic constants of the photocatalytic degradation reactions of several organic pollutants. We used first the simplified models and, afterwards, we refined our results with the complex model. Fig. 6 and Table 1 show the results in the case of 4-chlorophenol in terms of comparison between calculated (with the complex model) and experimental conversion of the organic reactant (we find $K_1 = 3.55 \times 10^{-11}$, $K_2 = 5.62 \times 10^{-11}$ and $K_3 = 1.02 \times 10^{-3}$).

We studied experimentally cases with c_0 = 100–1000 ppm, $\Phi_{\mathrm{liq}} = 15 \times 10^{-3}$–$45 \times 10^{-3}$ l/min, Φ_{gas} = 2 l/min, μ_v = 30 m^{-1}, σ_v = 120 m^{-1} and W_{LAMP} = 80 W.

Table 1
Comparison between theoretical values and experimental results

c_0 (ppm)	Φ_{liq} (cm^3/min)	Φ_{gas} (l/min)	Za experimental	Za theoretical
84.5	45	2	0.412	0.432552
105.6	25	2	0.568	0.630181
220.7	45	2	0.276	0.226634
755.8	15	2	0.33	0.267762
445.7	25	2	0.26	0.241455
50.7	45	2	0.621	0.589752
50.7	25	2	0.853	0.908264
219.9	45	2	0.326	0.227207
249.2	25	2	0.431	0.362591
654.5	20	2	0.2296	0.226421
763.7	9.5	2	0.393	0.404938

9. Conclusions

We set up a mathematical model in order to study and understand the behaviour of an annular fixed bed photochemical reactor. We consider only the case of single-lamp reactors, but the knowledge acquired will permit us to scale to the case of multi-lamp reactors, which are of industrial importance. Afterwards, we introduced two simplified models, which allowed us easier computational procedures.

We should stress two facts:

1. The chemical phenomena that occur at the surface of the catalyst, during catalytic photo-oxidation, are very complex and cannot be simulated by a Langmuir law as often assumed in the literature; the more complicated kinetic rate equation [4] should be employed. The use of Langmuir behaviour could be acceptable only at high concentration of pollutant, but it is not our case. At lower concentration, the profiles chemical rate R_A versus concentration c_L between Langmuir and Minero laws are considerably different. In particular, Minero law foresees the possibility of a maximum that is impossible with Langmuir's.
2. The radial dispersion is usually forgotten in chemical reactors, but here is an essential parameter in order to optimise the distribution of lamps in a commercial unit; unfortunately, until now, there is a lack of data in literature concerning this parameter.

For further reading see [7,8,12].

References

[1] G. Baldi, V. Specchia, Distribution and radial spread of liquid in packed towers with two-phase cocurrent flow: effect of packing shape and size, Quaderni Ingegnera Chimico Italiano, 7-8-9, (1976) 107–111

[2] J. Carberry, A. Varma (Eds.), Chemical Reaction and Engineering, Dekker, New York, 1992.

[3] A.E. Cassano, S. Whitaker (Eds.), Concerts and Design of Chemical Reactors, Gordon and Breach Science Publishers 1985.

[4] C. Minero, Kinetic analysis of photoinducted reactions at the water semiconductor interface, Catal. Today 54 (1999) 205–216.

[5] S. Mochizuki, T. Matsui, Liquid–solid mass transfer rate in liquid–gas upward cocurrent flow in packed beds, AIChE J. 24 (1978) 1138.

[6] F. Chiampo, Studio di cinetiche catalitiche in reattori polifasici, Master Dissertation, Politecnico di Torino, 1986.

[7] G.C. Rajnish, G.B. Raupp, Two-dimensional heterogeneous model for a reticulated-foam photocatalytic reactor, AIChE J. 46 (4) (2000) 829.

[8] G.B. Raupp, A.N. Jill, A. Suneetha, G.C. Rajnish, A. Rao, Two-flux radiation-field model for annular packed-bed photocatalytic oxidation reactor, AIChE J. 43 (3) (1997) 792.

[9] C. Renzi, Reattore fotocatalitico a catalizzatore supportato, Ph.D. Thesis, Politecnico di Torino, 1997.

[10] L.P. Reiss, Cocurrent gas–solid contacting in packed columns, Ind. Eng. Chem. Process. Des. Dev. 6 (1968) 486.

[11] M.Y. Saada, Chem. Ind. Genie Chem. 105 (1972) 1415.

[12] B.E. Serrano, H. De Lasa, Photocatalytic degradation of water organic pollutants. Kinetic modelling and energy efficiency, Ind. Eng. Chem. Res. 36 (11) (1997) 4705–4711.

[13] R. Siegel, J. Howell, Thermal Radiation Heat Transfer, Hemisphere, Washington, DC, 1992.

[14] G. Spadoni, E. Bandini, F. Santarelli, Scattering effects in photosensitized reactions, Chem. Eng. Sci. 3 (1978) 517–524.

[15] V. Specchia, G. Baldi, A. Giannetto, Ind. Eng. Chem. Process. Des. Dev. 17 (1978) 362.